Direct experimental determination of the tunnelling time and transmission probability of electrons through a resonant tunnelling structure

1991 J. Phys.: Condens. Matter 2 8969

(http://iopscience.iop.org/0953-8984/2/45/011)

J. Phys.: Condens. Matter 2 (1990) 8969–8975. Printed in the UK

LETTER TO THE EDITOR

Direct experimental determination of the tunnelling time and transmission probability of electrons through a resonant tunnelling structure

M Tewordt, V J Law, M J Kelly†, R Newbury, M Pepper,
D C Peacock†, J E F Frost, D A Ritchie and G A C Jones
Cavendish Laboratory, Madingley Road, Cambridge CB3 0HE, UK

Received 26 June 1990, in final form 5 September 1990

Abstract. A sharp step-like structure, which we see in the current–voltage characteristic of a laterally confined AlGaAs/GaAs resonant tunnelling structure, is a novel manifestation of a quantum effect arising when one-dimensional wires feed electrons into a zero-dimensional quantum box. We can analyse the data to deduce a tunnelling time, an inelastic scattering time and the transmission probability for electrons in this system. The height of the current steps, ΔI, gives the electron tunnelling time, τ_e, via $\Delta I = e/2\tau_e$, while the differential conductance gives the peak transmisssion probability, T_0, via $G \sim (e^2/h)T_0$. We must invoke inelastic scattering to explain the low value of $T_0 \sim 9\%$ obtained from the data, and so we find that tunnelling in our structure is sequential.

Since the fundamental work of Chang, Esaki and Tsu [1], introducing the resonant tunnelling structures (RTS), much effort has been devoted to increase our understanding of the detailed tunnelling process [2]. One of the controversial points in this discussion is the resonant or sequential nature of the transport in real RTS. Important physical parameters in RTS theory include the tunnelling time and the transmission probability. The times involved in the tunnelling process depend exponentially on the barrier widths, and have been determined experimentally in photoluminescence experiments [3]. The transmission probability $T(E)$ for an electron in an incoming plane wave state of energy E and below the top of the barrier, is almost always very small, except for certain discrete energies E_n where it is of order unity. In a solid, where inelastic scattering is always present, a plane-wave state for the incoming electron is inappropriate, and a wavepacket state must be used. As Stone and Lee [4] have shown, this has as a consequence that the transmission probability is decreased by a factor $(1 + \tau_e/\tau_i)^{-1}$, where τ_e is the characteristic tunnelling time of the electron through the double barrier (or elastic scattering time) [4], and τ_i is the inelastic electron scattering time in the semiconductor. To test this and other aspects of resonant tunnelling theory, appropriate experiments are needed.

In this letter we report an experiment in which we probe directly τ_e, τ_i and T_0, this last being the peak value of $T(E)$. The system used is a conventional AlGaAs/GaAs RTS, but with lateral confinement, leading to a zero-dimensional (0D) quantum box,

---

† Also at the GEC Hirst Research Centre, East Lane, Wembley HA9 7PP, UK.

separated by the barriers from two one-dimensional (1D) quantum wires. Both 1D [5–8] and 0D [9–11] semiconductor systems are of great current interest for the investigation of quantum transport, but only two 1D–0D–1D systems have so far been studied experimentally [9, 10]. Both Reed *et al* [9] and Smith *et al* [10] observed resonance-like structures in transport experiments which they interpreted as due to tunnelling through the 0D states from the 1D contact regions. However, we present and explain new data which clearly show sharp steps in the current–voltage characteristics as successive 0D electron states fall below the Fermi level in the 1D wire contacts. We explain this novel quantum effect with a simple theory, but include inelastic scattering [4], leading to the direct determination of τ_e, τ_i and T_0. Our results indicate that sequential tunnelling is dominant.

In our fabrication of the 1D–0D–1D system, we follow broadly the approach of Randall *et al* [12]. Small mesas are etched from a semiconductor multilayer, with ohmic top contacts. The lateral confinement of the carriers within the mesa is caused by Fermi surface pinning at the exposed surfaces. To provide vertical quantization, we use resonant tunnelling multilayers grown by molecular beam epitaxy. They were grown on n^+ (Si doped) substrates, and the layer sequence as grown consisted of: (i) 1 μm of GaAs, Si-doped to 10^{18} cm^{-3}, (ii) 5 nm GaAs (spacer), (iii) 5 nm AlGaAs (32% Al, barrier), (iv) 5 nm GaAs (well), (v) 5 nm AlGaAs (32% Al, barrier), (vi) 5 nm GaAs (spacer) and (vii) 1 μm of GaAs, Si-doped to 10^{18} cm^{-3} (top contact layer). Layers (ii) to (vi) inclusive are undoped. Small chips of this material were pre-etched with reactive ion etching (RIE) in a Plasma Technology RIE 80 system, using a $CH_4 : H_2$ process, at an etch rate of 20 nm min^{-1}: full details of this process have been published elsewhere [13]. The pre-etch reduces the top layer thickness to less than 0.3 μm: while the full thickness is useful in fabricating large area mesas, we use the pre-etched material to circumvent aspect ratio problems in the deep mesa etching of the very fine structures. With a modified Hitachi 800 series scanning electron microscope and polymethylmethacrylate (PMMA) resist, high resolution electron-beam lithography was performed to define both ensembles and isolated, small metallization dots on the surface, ranging in diameter between 2 μm and 0.15 μm. These dots serve the dual purpose of ohmic contacts and RIE etch masks. Three top metallizations were performed: (i) 50 nm AuGeNi, (ii) 20 nm NiCr and (iii) 110 nm Ag. The back contact to the substrate was formed by evaporating AuGeNi. These ohmic contacts were annealed with an optical rapid-thermal-annealer for 1 second at 400 °C. In the following step, the same RIE conditions were used to etch 0.5 μm deep columns, directly under the top ohmic contacts. Planarizing polyimide was spun around the columns, cured, and etched back with an oxygen plasma. Top contact pads, consisting of layers of Pd followed by Ag and Au, were formed by lift off. The back contact is fixed to a package using a conducting paint, and the top contact pads were then wire-bonded. Figure 1 shows an electron micrograph of typical etched columns, before the polyimide planarization and etch-back. Note the very smooth surface morphology. The important modifications to previous work [12] include: (i) very short spacer layers (to reduce space–charge band bending in the vertical direction), (ii) our etch gas, which seems to reduce surface damage and leave clean surfaces, (iii) different metal compositions in the ohmic top contacts and (iv) the pre-etch step already explained.

Low temperature current–voltage (I–V) and differential conductance–voltage ($\partial I/\partial V$–V) measurements were made in an Oxford Instruments TLM dilution refrigerator, the sample being immersed in the mixing chamber dilute phase at 30 mK. Standard DC and low frequency AC techniques were used, the latter with a modulation voltage of

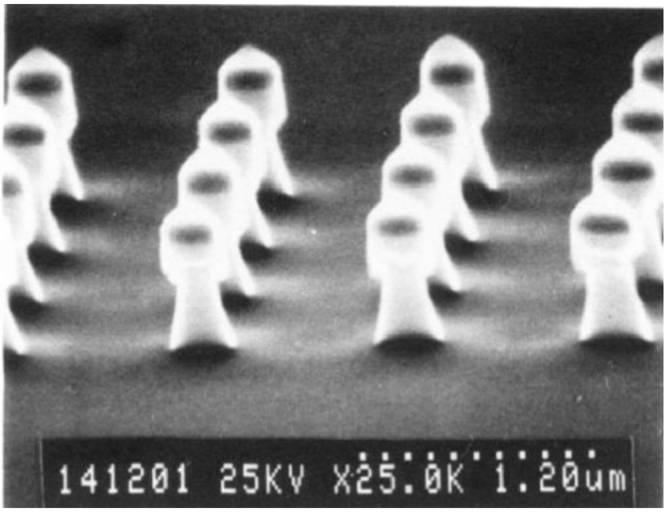

Figure 1. Free-standing columns of area 0.25 μm by 0.25 μm containing the laterally confined resonant tunnelling structures, etched with $CH_4:H_2$, using an AuGeNi/NiCr/Ag alloyed ohmic contact mask technology.

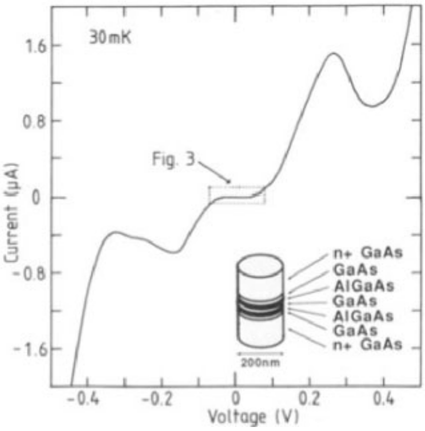

Figure 2. Current–voltage characteristics of a resonant tunnelling structure with a physical lateral size of 200 nm, as shown in the inset, for a mixing chamber temperature of 30 mK.

less than 100 μV. The *I–V* characteristic shown in figure 2 is from a set of 4 columns (each of area 0.2 μm by 0.2 μm). The main resonant tunnelling peak occurs in forward bias at 265 mV, which is nearly the same value as for larger mesas (i.e. with greater than 2 μm side). This indicates that the ohmic contacts are working well and that their contribution to the series resistance is small. Using the peak current density of 2.2×10^8 Am^{-2} obtained in the larger mesas, the peak current here (1.52 μA) implies an 'active area' of 0.007 $\mu\mathrm{m}^2$, which is only a fraction of the physical area (0.040 $\mu\mathrm{m}^2$) of a single column. This strongly suggests that we have lateral confinement, although it does not tell us how many columns are active: further evidence suggesting just one active

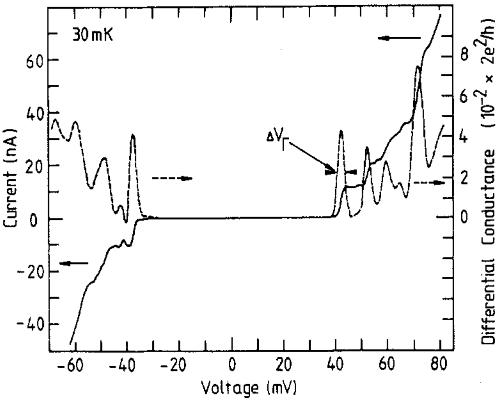

Figure 3. Expansion of the current–voltage (I–V) characteristics in figure 2 (full curve). Also shown is the differential conductance–voltage (G–V) characteristic in units of ($10^{-2}\,2e^2/h$) (broken curve). The value ΔV_Γ is the full width at half maximum of the G–V resonances, which give us the 0D-box state linewidths Γ via $\Gamma = e\Delta V_\Gamma/2$.

column is given below. We now focus on the bias up to 100 mV, where we observe fine structure just at the threshold of current: see figure 3 for the expansion of figure 2, where we have plotted the I–V (full curve) and $\partial I/\partial V$–V characteristics (broken curve). In the I–V plot we see that the current below a forward bias of 42 mV is essentially zero, but then rises abruptly to a plateau of 12 nA, which lasts for 10 mV until 52 mV bias, where another rise to a second plateau occurs, and so forth. At higher biases, this structure washes out. For negative bias, we observe a similar structure. In the $\partial I/\partial V$–V plot we see that the peaks, corresponding to the I–V step thresholds, have different maximum values and linewidths, and we observe a fine structure between the first two resonances, leading to negative differential conductance. For higher biases, a growing background comes in, which seems to be the cause for the smoothing out of the I–V structure. We note here that we have observed this structure at $T = 4.2$ K, but it is not as sharp.

To interpret our data, we introduce a simple model of a 0D quantum box with discrete energy levels connected by quantum wires having 1D electronic sub-bands. In analogy with transport in 1D systems studied earlier [6, 7, 10], we write the current for this system, at zero temperature, as

$$I = e\int_{E_{\rm f}-eV}^{E_{\rm f}} \sum_n N_n(E)v_n(E)T_n(E+eV/2)\,\mathrm{d}E. \tag{1}$$

Here $N_n(E)$ is the one-dimensional density of states of the nth 1D sub-band, and $v_{\rm n}(E)$ is the velocity of electrons at energy E in sub-band n. The $T_n(E + eV/2)$ term describes the sharply peaked energy dependence of the transmission through our double-barrier resonant tunnelling structure, taking into account the effect of half the applied bias in shifting the peak in transmission with respect to the energy levels in the source contact. In 1D quantum wires, the product $N_n(E)v_n(E) = 2/h$ is independent of energy and dependent only on Planck's constant, for whatever detailed form the band structure takes. For $T_n(E)$ we use the formula derived by Stone and Lee [4] for the transmission through a 0D-box resonance E_n of finite energy width Γ,

$$T_n(E) = T_{0,n}/\{1 + [2(E - E_n)/\Gamma]^2\} \tag{2}$$

with $T_0,n = \Gamma_{\rm e}/\Gamma$, $\Gamma_{\rm e} = \hbar/\tau_{\rm e}$, $\Gamma_{\rm i} = \hbar/\tau_{\rm i}$ (T_0, $\tau_{\rm e}$ and $\tau_{\rm i}$ as defined previously), and $\Gamma =$

$\Gamma_e + \Gamma_i$. Equation (2) is obtained by including inelastic scattering, leading to an expression for the transmission of an incident wavepacket on our double barrier structure. In the limit of no inelastic scattering, i.e. the resonant tunnelling limit (plane waves), this formula still applies, with $\Gamma = \Gamma_e$, and $\Gamma_i = 0$, resulting in $T_0 = 1$ for symmetric barriers. At the other extreme, the sequential tunnelling limit^2, we have $\Gamma_i \gg \Gamma_e$ and $T_0 = \Gamma_e/(\Gamma_e + \Gamma_i) \sim \Gamma_e/\Gamma_i = \tau_i/\tau_e$ becomes small. Assuming energy conservation, we obtain for each sub-band n, from equation (1), and using (2), a current contribution

$$I_n = \frac{2e}{h}\int_{E_f-eV}^{E_f} T_n\,(E + eV/2)\,\mathrm{d}E = \left(\frac{e}{h}\right) T_{0,n}\Gamma\left[\tan^{-1}\left(\frac{2[E_f + (eV/2) - E_n)}{\Gamma}\right)\right.$$
$$\left. - \tan^{-1}\left(\frac{2[E_f - eV + (eV/2) - E_n]}{\Gamma}\right)\right] \qquad (3)$$

leading for sufficiently small Γ to current steps of height

$$\Delta I = e\pi\Gamma_e/h = e/2\tau_e$$

for each n, which gives us the characteristic tunnelling time $\tau_e = 6.7$ ps, or the linewidth of the state $\Gamma_e = 0.1$ meV, using $\Delta I = 12$ nA for the first step ($n = 1$). Each time a new 2D state falls below the Fermi energy a further current step occurs so that the width, in bias, of the step is $\Delta V = 2\Delta E/e$, where ΔE is the difference between adjacent quantized 0D energy levels. To test this model, we have calculated the 1D-transmission probability $T(E)$ using as input the barrier and well widths, but also including the effect of the actual voltage drop across the structure under bias. From this we obtained a linewidth of the resonance of $\Gamma_e \sim 0.15$ meV ($\tau_e \sim 4.4$ ps) in good agreement with the experiment, which was relatively insensitive to slight changes in the thickness of one barrier (~0.5 nm) and applying a bias of ~50 mV. We note here, that we have measured a further device with exactly the same parameters as those above, except that the thickness of both barriers was reduced from 5 nm to 4 nm. As our model predicts, the step height ΔI is increased dramatically to 66 nA, which gives $\Gamma_e = 0.54$ meV ($\tau_e = 1.2$ ps). Here the calculated linewidth is $\Gamma_e = 0.86$ meV ($\tau_e = 0.76$ ps, or $\Delta I \sim 100$ nA).

In order to apply this model, we examine the data in more detail. The Fermi energy in the contacts is approximately 50 meV, whereas by considering the z-confinement, the lowest ground state in our system is calculated to be $E_0 = 72$ meV. A bias of 44 mV over the whole structure will reduce E_0 to the Fermi energy, and hence allow tunnelling. This agrees well with the experiment. In figure 3, in forward bias, we find for a width of the first step $\Delta E_1 \sim 6.25$ meV. For this value we calculate in a rigid-wall potential model a wall separation $a = 52$ nm using the formula $\Delta E_{\mathrm{RW}} = 3\hbar^2\pi^2/2m^*a^2$ for the separation of the first excited energy level from the ground state. This agrees reasonably with the implied conducting area derived above, which is much smaller than the physical dot area due to depletion and surface damage. We note here, that our high magnetic field 0D-box spectrum [15] shows some similarity to model calculations for potentials like ours [16]. Because of these considerations, we think that it is justified to assume that we observe only one active device.

An elegant approach to determine $T(E)$ and Γ is to measure the differential conductance $G = \partial I/\partial V$ as a function of the voltage. Differentiation of (3) yields

$$G = \frac{\partial I}{\partial V} = \frac{(2e^2/h)(\partial E/\partial eV)T_{0,n}}{[\![1 + \{2[E + (eV/2) - E_n]/\Gamma\}^2]\!]} = \left(\frac{2e^2}{h}\right)\left(\frac{\partial E}{\partial eV}\right) T_{0,n}$$

in resonance, with the peak transmission $T_{0,n}$ corresponding to the 0D-box state E_n, and

$(\partial E/\partial eV) \sim 1/2$. In figure 3, we find for the first resonance E_0 in forward bias a maximum of $G = 3.3\,\mu S = 0.043(2e^2/\mathrm{h})$, corresponding to $T_{0,0} = 8.6\%$. The full width at half maximum ΔV_Γ of this resonance, also shown in the figure, is related to the linewidth Γ via $\Gamma = e\Delta V_\Gamma/2$, and we find $\Gamma = 1.5$ meV. From this, we obtain directly $\Gamma_i = \Gamma - \Gamma_e \sim 1.4$ meV, corresponding to $\tau_i \sim 0.5$ ps, indicating strong inelastic scattering. In this situation, tunnelling is sequential, not resonant [2]. The small value of T_0 cannot be explained solely by asymmetric barriers or the effect of an applied bias within the resonant tunnelling model since $T_0 = T_{\mathrm{min}}/T_{\mathrm{max}}$, where T_{min}, T_{max} are the transmission probability of the thinner and thicker barrier respectively. The error of the given barrier thickness is at most 10% from TEM data, and so we have a deviation of T_0 from unity of at most 40% in forward bias [14, 17]. As can be shown with simple calculations, the assumption of a high series resistance to the RTS from the ohmic contacts or leads can be ruled out as an explanation for the small T_0, since it would not explain the broad linewidths observed. For the resonances at higher bias we find similar, though not identical, results for T_0 and Γ as for lower biases. However, the positive background for higher voltages also indicates that $T(E)$ is not governed solely by the 0D-box states. It is interesting to note that the peak conductance for the second device (first resonance) with the 4 nm barriers is increased to $G_0 \sim 5\,\mu\mathrm{S} \sim 0.064\,(2e^2/h)$, corresponding to $T_0 \sim 13\%$, while $\Gamma \sim 3.5$ meV, as expected from the thinner barriers. A detailed discussion of all these phenomena, along with the negative conductance features, for these and other devices, will be presented in further work [15].

We suggest that the scattering mechanism leading to τ_i may be single-optical-phonon emission of LO phonons with $E_{\mathrm{LO}} = 36$ meV. This is possible, since the bias is always greater than 40 mV for our structures. Single-optical-phonon emission has recently been studied in a system qualitatively similar to ours [18] and the typical inelastic scattering times τ_i found for this effect were indeed between 0.2 ps and 0.5 ps (dependent on the electron energy and the Al content). Finally we would like to point out that the Coulomb blockade effect cannot be ruled out as an explanation for our data, but our high magnetic field experiments show first-order changes in the step sizes with bias which are consistent with an electric sub-band model [11].

In conclusion, we have found a novel quantum effect in laterally confined AlGaAs/GaAs RTS, which manifests itself in a sharp step-like structure in the current–voltage characteristics. Within a model of 1D–0D–1D electron states we are able to explain the structure and to determine directly the time τ_e for an electron to pass through the double barrier structure. Taking inelastic scattering into account, we are able, for the first time, to determine directly the transmission probability, and to estimate the inelastic scattering time τ_i. Finally, transport in our system is predominantly by sequential tunnelling. Further work, both experimental and theoretical has to be done to understand the detailed scattering mechanism and the transmission probability of the system.

We thank L Martin-Moréno, C G Smith and S Datta for helpful discussions. We are also grateful for the technical assistance of B K Papworth and P Booth. MT acknowledges a grant from the Commission of the European Communities and earlier partial support from the Dr Carl Duisberg Stiftung. MJK is supported in part by a Royal Society/SERC Industrial Fellowship. This work is also supported by the SERC.

References

[1] Chang L L, Esaki L and Tsu R 1974 *Appl. Phys. Lett.* **24** 593–5

[2] For a review see Mendez E E 1987 *Physics and Applications of Quantum Wells and Superlattices* ed E E Mendez and K von Klitzing (New York: Plenum) 159–88

[3] Tsuchiya M, Matsusue T and Sakaki H 1987 *Phys. Rev. Lett.* **59** 2356–59

[4] Stone A D and Lee P A 1985 *Phys. Rev. Lett.* **54** 1196–99

[5] Thornton T J, Pepper M, Ahmed H, Andrews D and Davies G J 1986 *Phys. Rev. Lett.* **56** 1198–200

[6] Wharam D A, Thornton T J, Newbury R, Pepper M, Ahmed H, Frost J E F, Hasko D G, Peacock D C, Ritchie D A and Jones G A C 1988 *J. Phys. C: Solid State Phys.* **21** L209–13

[7] van Wees B J, van Houten H, Beenakker C W J, Williamson J G, Kouwenhoven L P, van der Marel D and Foxon C T 1988 *Phys. Rev. Lett.* **60** 848–50

[8] Smith III T P, Arnot H, Hong J M, Knoedler C M, Laux S E and Schmid H 1987 *Phys. Rev. Lett.* **59** 2802–5

[9] Reed M A, Randall J N, Aggarwal R J, Matyi R J, Moore T M and Wetsel A E 1988 *Phys. Rev. Lett.* **60** 535–8

[10] Smith C G, Pepper M, Ahmed H, Frost J E F, Hasko D G, Peacock D C, Ritchie D A and Jones G A C 1988 *J. Phys. C: Solid State Phys.* **21** L893–8

[11] Hansen W, Smith III T P, Lee K Y, Brum J A, Knoedler C M, Hong J M and Kern D P 1989 *Phys. Rev. Lett.* **62** 2168–71

[12] Randall J N, Reed M A, Moore T M, Matyi R J and Lee J W 1988 *J. Vac. Sci. Technol.* **B6** 302–5

[13] Law V J, Jones G A C, Peacock D C, Ritchie D A and Frost J E F 1989 *J. Vac. Sci. Technol.* **B7** 1479–82

[14] Syme R T private communication
Stobbs W M private communication, and to be published

[15] Tewordt M *et al* to be published

[16] Robnik M 1986 *J. Phys. A: Math. Gen.* **19** 3619–30

[17] Ricco B and Azbel M Ya 1984 *Phys. Rev.* B **29** 1970–81

[18] Heiblum M, Galbi D and Weckwerth M 1989 *Phys. Rev. Lett.* **62** 1057–60